In situ stress measurements during anodic dissolution of cold spray AA6061 coating

by

Prashant Gargh

A thesis submitted to the graduate faculty

in partial fulfillment of the requirements for the degree of

MASTER OF SCIENCE

Major: Mechanical Engineering

Program of Study Committee:
Pranav Shrotriya, Major Professor
Jonghyun Lee
Ikenna C. Nlebedim
Shan Hu
Chao Hu

The student author, whose presentation of the scholarship herein was approved by the program of study committee, is solely responsible for the content of this thesis. The Graduate College will ensure this thesis is globally accessible and will not permit alterations after a degree is conferred.

Iowa State University

Ames, Iowa

2021

TABLE OF CONTENTS

Page

LIST OF FIGURES iii

LIST OF TABLES iv

ACKNOWLEDGMENTS v

ABSTRACT vi

CHAPTER 1. INTRODUCTION 1
1.1 Corrosion: Need for Coatings 1
1.2 Coatings 2
1.3 Thermal Spray Coatings 3
1.4 Additive Manufacturing 4
1.5 Working Principle: How does Additive manufacturing work in metals 5
1.6 Cold Spray Technique 6
1.7 Advantages and Challenges of cold spray process 7
1.8 Comparison of cold spray with traditional thermal spray techniques 8

CHAPTER 2. INSITU STRESS MEASUREMENT AND CORROSION RESPONSE OF COLD SPRAY AA 6061 COATINGS 9
2.1 Introduction 9
2.2 Experimental Procedure 12
2.3 Results 14
2.3.1 Microstructural Characterization 14
2.3.2 Potentiodynamic Polarization Scan With Respect To Exposure Time 16
2.3.3 Measurement Of Force Per Width During Open Circuit Potential Condition 19
2.3.4. In-Situ Stress Measurement During Anodic Dissolution At 0.3v Above OCP With Respect To Exposure Time 20
2.3.5 Corroded Surface After Electrochemical Measurements 22
2.3.6 Comparison Of Cold Spray Coating After Exposure Using Energy Dispersive X-Ray Analysis 24
2.4 Supplementary Information 26

CHAPTER 3. CONCLUSION 28
3.1 General Conclusion 28
3.2 Future Work 29

REFERENCES 30

LIST OF FIGURES

Page

Figure 1.1: Schematic of thermal spray coating process (adapted from [20][21]). 3

Figure 1.2 Schematic representation for additive manufacturing working principle(adapted from[28][40]). 5

Figure 1.3 Schematic representation of cold spray additive manufacturing process comprising of two powder feeds and two sources of gases were used(adapted from [44]). 6

Figure 2.1 SEM micrograph of AA 6061 cold spray coating on AA2024 substrate as received condition (a) top view (b) cross section view 15

Figure 2.2 Potentiodynamic polarization curves of CS AA6061 coated on AA2024 coupons in 3.5wt. % solution using 1mV/sec scan rate (i) immediately upon exposure and (ii) 2 hours wait in 3.5% NaCl solution. 18

Figure 2.3 Change in force along the width during open circuit potential(OCP) scan for AA 2024. 20

Figure 2.4 Force per width (black) and current density (dotted red) during Potentiostatic polarization scan at 0.3V above OCP for (a) immediate and (b) 2 hrs. wait. 21

Figure 2.5 SEM micrograph of AA6061 cold spray coating on AA2024 substrate after anodic dissolution condition (a) top view (b) cross section view (crack propogation) 23

Figure 2.6 Energy-dispersive X-ray spectroscopy (EDS) maps of the cold spray coating showing the elemental maps distribution for Al, Si, Mg, Na, Cl and O (a) top view (b) cross section view 25

LIST OF TABLES

Page

Table 2.1: Chemical composition for AA 6061 and AA 2024 13

Table 2.2 EDS analysis showing the mass percentage of AA 6061 at four regions. 16

Table 2.3: Electrochemical parameters obtained using Tafel extrapolation method. 18

ACKNOWLEDGMENTS

It is with immense gratitude that I acknowledge the support of my advisor, Dr. Pranav Shrotriya, for his guidance and sustained support extended to me during this precious time in my graduate studies at Iowa State University. His direct supervision motivated me to utilize my energy and efforts throughout the course of this research.

I would like to utilize the opportunity to express and extend my thanks and sincere gratitude to my committee members Dr. Jong Lee, Dr. Ikkena Nlebedim, Dr. Shan Hu and Dr. Chao Hu for serving on my thesis committee throughout the course of this research.

In addition, I would also like to thank and appreciate my friends, colleagues, the department faculty and staff for making my time at Iowa State University a wonderful experience, without whom, this thesis would not have been possible.

Above all, I want to extend my gratitude to my parents and my wife for their love, encouragement and sustained support throughout the years of my schooling and valued moments through college while pursuing undergraduate and graduate education in engineering.

ABSTRACT

In this study, corrosion performance of AA 6061 coating deposited on AA 2024 substrate using the cold spray(CS) deposition technique was investigated.AA 6061 and AA 2024 alloys are used widely in aircraft and marine industries. As received CS coating of 6061 is dense film covered with spherical particles that have equiaxed grain structure in the center but elongated grains due to plastic deformation near the particle edges. Elemental analysis indicates that grains in the center of particle have the same compostion as 6061 alloy but the grains near the boundary are richer in silicon and magnesium. Electrochemical measurements including open-circuit potential, potentiodynamic, and potentiostatic polarization measurements in simulated salt water solution were carried out to examine the corrosion performance. Simultaneously, film force/thickness evolution during exposure to corrosive solution was measured using curvature interferometry technique. The results showed that exposure to 3.5wt% NaCl solution is associated with development of large compressive stresses on the sample surface. Examination of the surface after the exposure shows only localized corrosion and therefore, measured stress may be associated with relaxation of coating induced residual stresses in the film through dissolution of tensile stress loaded region. While anodic dissolution at +0.3V above OCP in salt solution leads to formation of large pits and development of tensile stresses. The microstructure analysis of the corroded surfaces show pits with small opening but large subsurface volumes as well as formation of silicon and oxygen rich film on the particle boundaries. The pits have the same dimensions as particles indicating complete consumption of the film particles during dissolution. In addition, subsurface cracks and extensive corrosive attacks along the particle boundary is observed below the pit openings. The formation of silicon rich oxide films near the particle boundaries and the propagation of sub-surface corrosive attack along the particle

boundary suggests that the processing induced compositional difference between paricle center and boundary may have resulted in the observed localized corrosion.

CHAPTER 1. INTRODUCTION

1.1 Corrosion: Need for Coatings

Corrosion of metals in seawater and marine environment is responsible for surface damage and deterioration of structures in shipping and marine industries. According to the National Association of Corrosion Engineers (NACE) [1], corrosion is defined as "the deterioration of a material, usually a metal, that results from a chemical or electrochemical reaction with its environment." It is necessary to prevent the material from the corrosive environment by identifying the reactions occurring between the surface and its environment. Then identify steps to reduce it so that it could thus lead to longer material life and higher corrosion resistance[2]. Based on a recent study from the NACE, they estimated losses of US$ 2.5 trillion globally due to corrosion [3]. There has been a great interest among material scientists to protect existing materials from corrosion[4–6]. In general, the formation of an electrochemical cell causes corrosion of metal[7]. A corrosion reaction can occur in any electrochemical cell when five necessary factors are present: the anode, cathode, electrolyte, electrical connection between anode and cathode, and a potential difference between anode and cathode[7][8]. However, the problem of localized corrosion is still a challenging field.

Aluminum alloys (AA) are extensively used in the automobile, marine, and aerospace industries. Due to its remarkable characteristics such as strength to weight ratio, toughness, corrosion and oxidation resistance, and flexible workability, this alloy can be fabricated in various shapes providing an excellent structure finish. Thus, aluminum alloys are best suitable for aircraft and marine industry applications due to their lightweight structure, low-cost maintenance, and operational costs[9]. In general, aluminum and its alloys form a protective oxide film on the surface under normal atmospheric conditions[10]. However, exposure to

specific environments such as halides could cause the local breakdown of this non-uniform passive film, forming an active site for localized corrosion [11,12]. Due to impurities or the addition of intermetallic in the metal alloys, the chemical composition plays a vital role in identifying the corrosive environment. The effect of major alloying elements such as the presence of copper in AA 2024 or silicon and magnesium in AA 6061 can contribute to higher strength, low melting point, increase in fluidity, and better heat-treatability[13]. However, these alloying elements in the presence of conductive environments (e.g., NaCl solution) can also contribute as local cathodic sites forming a corrosion cell with the nearby surface, causing dissolution of the metal alloy. This localized type of corrosion is generally referred to as pitting or galvanic corrosion [10–15]. Therefore, the most common solution available to prevent corrosion is to apply coatings on the material surface.

1.2 Coatings

Coatings on the metal surface have become widely popular due to technological advancements in recent years. They act as a barrier between the metal and the environment, which helps in reducing the degradation of the material surface, reduces operational costs, and extends their life[16]. A wide variety of pre-surface treatments[17] and deposition of coating methods[18] have been studied to increase corrosion resistance in aluminum alloys. Several coating methods exist in today's world that could be applied to the surface based on the application used[17]. Coatings were applied based on the application of the material; therefore, the bonding mechanism of the coatings and the substrate were given preferential importance. The need for environment-friendly coatings, reliable and low-cost, less complex processes has led to the evolution of spray-based coating techniques in recent years[18].

1.3 Thermal Spray Coatings

The thermal spray coating process utilizes the coating material in the wire or powder form (molten or semi-molten form), also referred to as feedstock powder, sprayed onto the material surface referred to as substrate using a nozzle gun. Varying high-velocity rates in the presence of high-pressure compressed gases, such as helium, nitrogen, argon, propane, air, to name a few, can be used in thermal spray coatings [19]. The temperature variation required to molten the coating material can be achieved chemically or electrically. The substrate is perpendicular to the nozzle gun when sprayed, forming a deposit on the substrate. When in a molten state, the powder particles undergo plastic deformation upon impact to the surface, also referred to as splats.

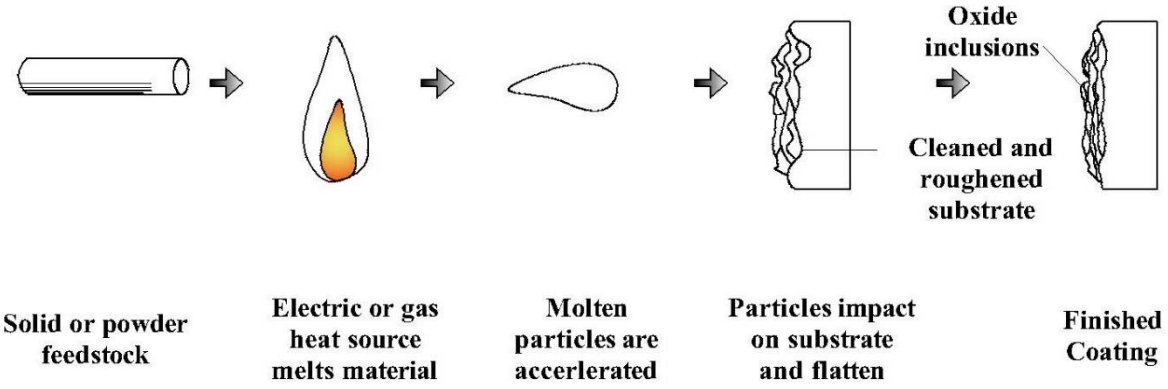

Figure 1.1: Schematic of thermal spray coating process (adapted from [20][21]).

Using thermal spray technique coatings of varying thickness from 50µm - 2500 µm[19] could be achieved[22]. Various parameters can affect the thermal spray processes, including particle size, particle velocity, temperature, to name a few. The advancement and need of thermal spray coatings have expanded due to its advantages and growing demand, especially in

aerospace, energy generation, and automotive industries[23][24]. Many studies have shown that thermal coatings have been an effective choice for repairing worn areas in components due to their application at local level areas such as turbine blades and engine blocks. Thermal spray coatings allow increased repair capabilities providing durability, improving performance, and longer service life.

1.4 Additive Manufacturing

Additive manufacturing(AM) is "the process of joining materials to make parts from 3D model data, using layer upon layer, as opposed to subtractive manufacturing and formative manufacturing methodologies" according to ISO/ASTM [25,26]. The addition of layer upon layer of the material helps fabricate self-supporting complex parts manufactured using this technique[27]. This method is applicable to the following classes of materials, i.e., metals, polymers, ceramics, and biomaterials[28–32]. A solid model was designed utilizing computer-aided design(CAD) software and translated into a genuine part[26]. In recent years, additive manufacturing has spread its horizons in a wide variety of industries. The benefit of extensive customization has led to immense growth in real-life industrial applications such as aerospace, automotive, medical, architecture, and defense.

The demand for low-volume manufacturing of parts can result in potential cost and time savings with complete flexibility than high-cost conventional mass manufacturing[33]. AM offers broad advantages. Some of the significant advantages of AM are: higher accuracy, customization of part design or complex geometry, waste reduction, cost savings, elimination of the need for tooling, optimization of parts, reduction in raw material usage, ease of sharing the digital design, reduces the risk of inventory, and flexibility to fabricate parts reducing carbon footprint [33–37].

1.5 Working Principle: How does Additive manufacturing work in metals

Figure 1.2 shows the working principle for additive manufacturing in metals. With computer-aided design (CAD) software, almost any part can be designed and converted into the desired standard file format, e.g., .stl format, then sent to an additive manufacturing device for fabrication. Further, the shape of the designed part is then built-in 2-D layers, which are stacked upon each other[38]. This can be done either point by point or layer by layer[29]. Various types of additive manufacturing processes for metals are available. However, they can be broadly categorized into types of processes used, i.e., source of heat or energy such as electron beam, laser, or arc [39], and types of raw material used, such as solid-based, liquid-based, and powder-based[29].

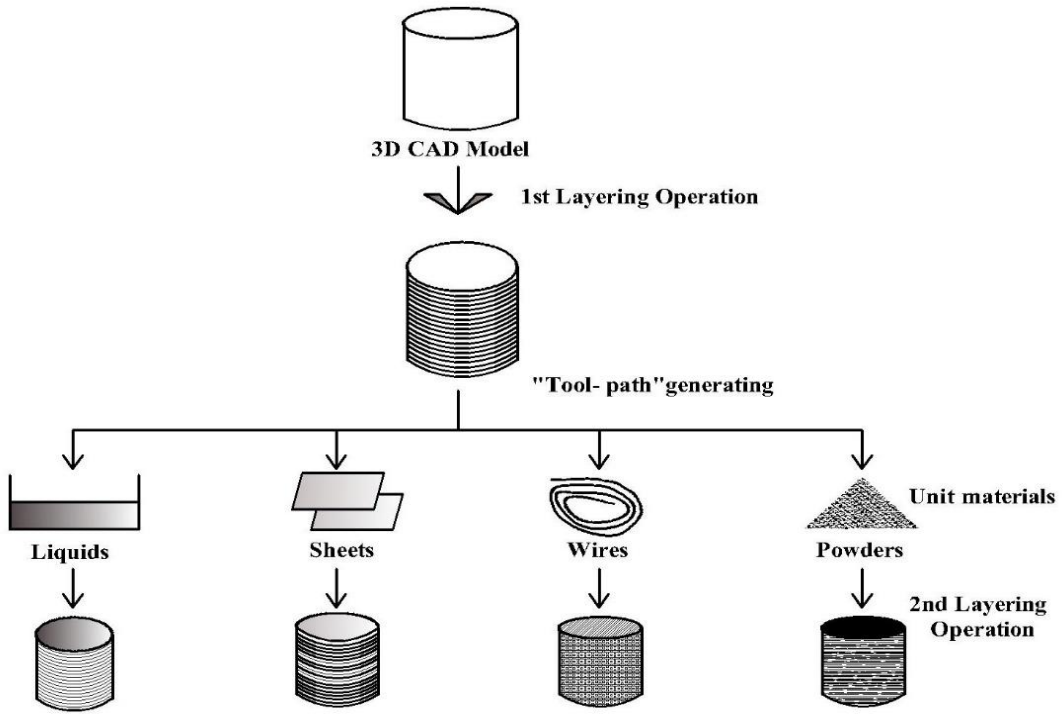

Figure 1.2 Schematic representation for additive manufacturing working principle(adapted from[28][40]).

1.6 Cold Spray Technique

The first discovery of the cold spray process was at the Institute of Theoretical and Applied Mechanics of the Russian Academy of Sciences(ITAM of R.A.S.) in Novosibirsk, Russia, in the 1980s [41][42]. Cold Spray (CS) coatings are created using solid powder particles of size range 5-100 μm when accelerated through a nozzle jet, in the presence of working gas, at supersonic speeds of around 300-1200 m/sec, at temperatures below the melting point of the material. Upon impacting the substrate, the powder particles experience elastic-plastic deformation forming dense and strong bonding due to splats formation on the surface [43].

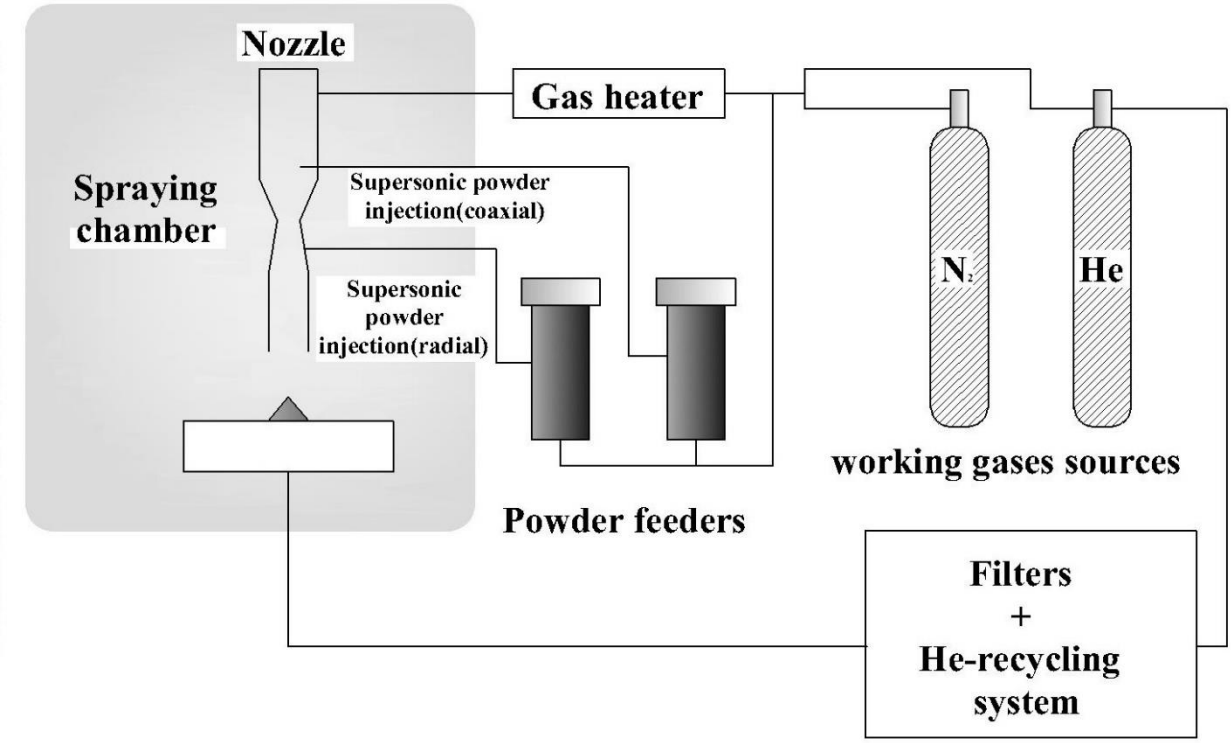

Figure 1.3 Schematic representation of cold spray additive manufacturing process comprising of two powder feeds and two sources of gases were used(adapted from [44]).

A wide variety of experimental research has been done in recent years to study and improve the bonding mechanisms for the substrate and coating done by the cold spray process using various materials [45–50].

1.7 Advantages and Challenges of cold spray process

Based on current research, which enabled the CS process to become one of the popular methods in additive manufacturing. Some of the benefits include[51–54] :

(i) No phase change of materials.

(ii) It can be used to deposit temperature/oxygen-sensitive materials

(iii) High mechanical properties and deposition rate

(iv) Lower oxide content

(v) Reduces wastage, cost and promotes dimensional restoration.

Despite enormous studies showing benefits of using the cold spray additive manufacturing technology, there are still certain challenges of the CS additive manufacturing process[55–57]:

(i) Lower geometrical precision and dimensional accuracy

(ii) Formation of voids

(iii) Formation of residual stresses on the part

(iv) Surface finishing

(v) Process parameters such as thickness, scan speed, and building direction

(vi) Additional cost for training and skills

1.8 Comparison of cold spray with traditional thermal spray techniques

One of the key advantages of using the CS coating technique is that the coating powder is not melted [58] and operated at much lower temperatures than their melting point. Therefore this process does not require melting of the powder. Whereas in thermal spray technique, the sprayed material is melted by using either electrical or chemical energy. CS technique uses kinetic energy due to the type of converging-diverging nozzle used in this process, causing the particle spray velocities around 500-1000m/sec and reduces the consumption of the gas, rather than thermal energy for deposition.

CHAPTER 2. INSITU STRESS MEASUREMENT AND CORROSION RESPONSE OF COLD SPRAY AA 6061 COATINGS.

2.1 Introduction

Aluminum alloys have been extensively used due to their excellent workability and high strength. Nevertheless, they possess the inability to provide sufficient protection in alkaline environments. The aluminum metal forms a thin, dense, passive layer of aluminum oxide (Al_2O_3) due to higher oxygen affinity. This oxide layer formed protects the aluminum surface, thus exhibiting corrosion resistance. However, under corrosive environments (such as halides), this passive oxide film could break, resulting in localized corrosion due to adsorption of Cl^- [59], leading to the initiation of pitting corrosion. In AA 6061, the corrosion susceptibility could be attributed to the alloying elements present[60].

Cold spray (CS) coatings are an emerging method in fabrication and repair for complex structures relative to other coating techniques[61]. Because of the lower application temperatures and deposition in solid-state compared to traditional thermal spray techniques, localized corrosion repair using cold spray method for complex geometric components, thus providing savings worth millions of dollars[62–65]. It is essential to choose a suitable coating material based on the substrate and the type of application.

The bonding mechanism between the CS particles and the substrate is dependent upon splats interlocking [66]. Using the CS process, these coatings can offer unique advantages: high density[65], reduced fatigue life[67], high corrosion resistance[65][67], increase in strength and hardness when applied to the substrate[65], good adhesion on the coating-substrate interface[68], compressive residual stress on the substrate[65], high deposition efficiency on metal alloys and composites[43,65,69]. Furthermore, the CS process could form a single-layer, which helps

achieve better adhesion to the surface and lower porous coating structure[70], and also multiple layer deposition of particles, providing denser structure with a higher modulus of elasticity [65][70].

In CS coatings, optimizing the particle size, impact velocity, gas pressure, and gas temperature is necessary for uniform deposition on the substrate[71]. The higher kinetic impact could break the oxide layer and cause splats formation on the substrate. These splats experience a tensile effect. Due to which the substrate experiences a compression effect immediately upon impact[72]. However, due to higher velocity impact of powder particles in CS technique and difference in coefficient of thermal expansion of coating and substrate causes an increase in residual stress[73–76]. This increase in residual stresses is a cause of concern. Various techniques such as layer removal technique[77][78], X-ray diffraction[73,76,79], neutron-diffraction[80], curvature measurement[81,82] have been used to measure residual stress and their nature(tensile or compressive) on the coatings and substrate. The nature of residual stress (tensile or compressive) on the coatings could cause cracking or delamination, which could result in the failure of coatings [72].

Marzbanrad et al. investigated the residual stress evolution due to CS coating of AA7075 on magnesium alloy substrate using a parametric study. They found that the temperature and pressure of gas used in the cold spray process significantly influence the residual stress [83]. One of the primary reasons for using aluminum alloys cold spray coatings is that it allows repairing and protecting aluminum(Al) components rather than scrapping and also allows reconditioned for existing components[28].

Ghelichi et al. [84] studied the fatigue strength of AA 5052 coated with CS pure Al and AA 7075. Their results show that the samples coated with CS AA 7075 had lower compressive residual stress on substrate AA5052, showed higher fatigue life, and cause an improvement of overall strength by up to 30% due to deposition of higher strength material by the CS process. In addition, coating parameters and material properties also contribute to improving the fatigue life of the part. This is an important observation, which could be helpful for real-world applications where complex structures cannot withstand fatigue and can help increase their long-term life. Cavaliere et al. [58] repaired V notch on AA 2099 substrate using CS coating of AA 2198 and AA7075. The results showed that crack resistance in the aluminum alloy panel increased six-fold, thus providing higher fatigue life. Incorporating α-Al_2O_3 in pure Al for CS coatings, which not only reduces the porosity but also allows an increase in adhesive and tensile strength[85].

Moridi et al. [86] studied the effect of coating similar AA material using the high-pressure cold spray technique. Rotating bending tests were performed on as-received samples and coated samples. The results revealed that compressive residual stress from CS coating caused a 14% increase in fatigue strength. However, numerous studies showed that under the influence of corrosive environments containing halides such as NaCl solution than in air, the fatigue life of AA6061 significantly reduced [87–89]. Consequently, the environment plays a vital role in acting as a catalyst to exhibit corrosion. Due to exposure in a higher corrosive environment, it is assumed that the thickness of the CS coating is reduced layer by layer removal occurs, which causes relaxation inside the structure, leading to a higher probability of failure[90].

The corrosion behavior of CS coatings on metallic substrates has been extensively investigated [91–94]. Rokni et al.[95] studied the CS coating of CS AA 7075 powder deposition on AA 7075 substrate. They found that the decrease in hardness along the thickness as the size of

local grains was comparatively smaller near the substrate than the CS coating surface. A larger grain size could also influence the porosity in the coating. In chloride solutions, the passive film breakdown occurs, causing chloride ions adsorption, leading to susceptibility to pitting corrosion[96].

Work done by Deforce et al. proposes a low-cost solution for corrosion protection by cold spraying aluminum powder on magnesium alloys. In this work, they evaluated them by performing mechanical and corrosion testing of Al-5 wt. % Mg, pure Al (99.5 wt. %), high purity Al (99.95 wt. %), AA 5356, and AA 4047 materials coated on ZE41A-T5 Mg alloy substrate. Based on the results obtained, they concluded that Al-5 wt. % Mg resulted in high hardness and low galvanic current than the others. This is because some elements could reduce the detrimental effect of others in the metal alloy[97].

With aluminum being a chemically active material, the instability of aluminum components in seawater environments provides us with evidence to estimate the corrosion behavior of AA. In this current work, the objective is to investigate the corrosion response of cold spray AA 6061 coatings on AA 2024 substrate in 3.5 wt.% NaCl solution and measurement of force per width using phase-shifting curvature interferometry. SEM imaging and EDS analysis of the corroded surface were performed to identify the type of corrosion, such that their use could extend to real-life applications.

2.2 Experimental Procedure

AA 6061 powder particles were cold sprayed (CS) on the AA 2024 substrate. These specimens were as received in the sheet size for roughly 10 inches * 5 inches. The chemical composition for elements in AA 6061 and AA 2024 are shown in Table 1.

Table 2.1: Chemical composition for AA 6061 and AA 2024

Elements	Si	Fe	Cu	Mn	Mg	Cr	Zn	Ti	Unspecified	Al.
AA 6061	0.4-0.8	0.7	0.15-0.40	0.15	0.8-1.2	0.04-0.35	0.25	0.15	0.05-0.15	Rem.
AA-2024	0.5	0.5	3.8-4.9	0.3-0.9	1.2-1.8	0.1	0.25	0.15	0.05-0.15	Rem.

The rectangular coupons were cut approximately to size 20 mm * 30 mm from the acquired specimens such that these coupons do not bend. The rectangular coupons were polished on the substrate side using silicon carbide grit papers up to 1200 grit grade. The final polishing was done using 1µm colloidal silica suspension and diamond paste to obtain a mirror finish. The coupons were polished using ethyl alcohol to prevent the formation of any oxide layer. The coupons were gently cleaned/rinsed/ using ethanol and dried in warm air after every change of grit paper to avoid contamination while polishing. All the coupons were sonicated in an acetone bath for 20 minutes, followed by ethyl alcohol and air-dried.

The electrochemical measurements were performed on the cold spray 6061 coating side using GAMRY® Ref 600 Potentiostat at ambient conditions. Standard 3-electrode cell set up was used with Ag-$AgCl_2$ as reference electrode, Pt wire was used as the counter electrode, and AA 6061 CS coating on substrate 2024 coupons as the working electrode. The electrolyte used was a 3.5% NaCl aqueous solution (pH 7.85) prepared with deionized water at room temperature. The working electrode area was approximately 2.4cm^2 with the dimensions of (2.4cm*1 cm) for all coupons. We chose the operating potential at approximately +0.3V above open circuit potential to monitor the film stress and currents during anodic dissolution using electrochemical measurements.All the potentials described in this work are with respect to reference electrode Ag-$AgCl_2$.

This study used an in-situ stress measurement by utilizing the phase-shifting curvature interferometry technique[82]. A detailed description of this technique has been mentioned elsewhere[81][82][98]. This method of measuring the curvature change on the sample surface to measure the force along the thickness during the corrosion of CS coating was monitored. Also, the Stoney thin-film approximation holds true as the AA 6061 CS coating and AA 2024 thickness are smaller in lateral directions. The coating thickness is comparatively smaller than substrate thickness, as shown in fig.2.1(b)[99].

Due to the ongoing electrochemical reactions, the change in curvature causes the evolution of stresses occurring inside the coupons were measured such that uniformity of the curvature was assumed, and the development of stresses due to CS coating material dissolution was examined in real-time.

This study comprehensively examined the morphology of CS-coated coupons by using scanning electron microscopy (SEM, FEI Quanta 250 FE-SEM) combined with Energy Dispersive X-ray Spectroscopy (EDS) to determine. (i) The initial condition of the CS coating, (ii) To characterize the type of corrosion on the CS coating, (iii) The extent and depth of crack propagation, (iv) The effect of anodic current due to electrochemical reactions, and (v) Other intrinsic features on and along with the thickness of the surface.

2.3 Results

2.3.1 Microstructural Characterization

2.3.1.1 As Received Condition

Fig. 2.1 shows the backscattered SEM micrographs for the cold spray AA 6061 coating and a cross-section view of cold spray AA 6061 coated on AA 2024 substrate in as-received

condition. Fig 2.1(a) shows AA-6061 particles: (1) were deposited perpendicular to the spray direction, (2) have a combination of small and large particles with irregular spherical shape type morphology, and (3) are plastically deformed locally due to high-speed impact on the substrate using CS technique; thus the CS coating remains bonded to the surface.

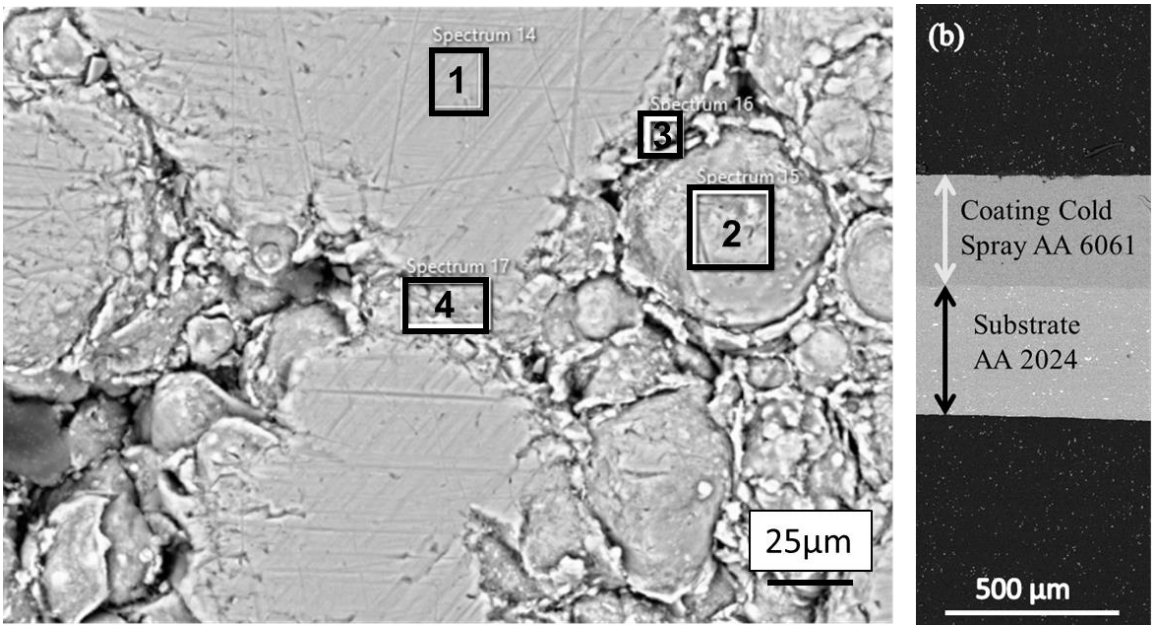

Figure 2.1 SEM micrograph of AA 6061 cold spray coating on AA2024 substrate as received condition (a) top view (b) cross section view

According to the literature, similar grains were observed for AA 6061 as received powder [100][101], seen in the CS coating. The top layer of the cold spray coating contains discrete porous areas near grain boundaries with a clear inhomogeneous deformation of powder particles in the structure. These non-uniform depositions allowed some powder particles to not adhere completely to the layered coating surface and some amount of interparticle voids and porosity on the coating surface. This indicates that those sites could be highly receptive towards corrosion

attack, represented by uneven mismatch areas, and are likely to cause poor corrosion resistance. Fig 2.1(b) shows the cross-section view of the cold spray AA 6061 coating (top) and AA 2024 substrate (bottom) bonded together, presenting excellent adhesion characteristics, dense coating structure and does not provide any evidence of cracks and pores. The coating thickness is approximately 330 ± 5 µm, whereas the substrate AA 2024 thickness is approximately 373.7 ± 5 µm.

Table 2.2 EDS analysis showing the mass percentage of AA 6061 at four regions.

Spectrum Label	**O**	**Mg**	**Al**	**Si**	**Fe**	**Cu**	**Total**
Spectrum 1/Flat region	2.15	0.90	95.66	0.82	0.19	0.27	100.00
Spectrum 2	2.48	0.94	95.15	0.98	0.18	0.27	100.00
Spectrum 3	9.43	0.95	85.15	4.29	0.18	0.00	100.00
Spectrum 4/Flat region	3.86	0.87	93.31	1.57	0.16	0.23	100.00

Table 2.2 compares the chemical composition obtained for the as-received coupon for two regions (i) Al particle powder surface and (ii) particle boundary(PB) as highlighted in figure 2.1(a) obtained using Energy-dispersive X-ray spectroscopy (EDS). The EDS analysis confirms that the particle boundaries have a much higher amount of segregation of Si, Fe, Mg, and O_2 and reduced aluminum content[101].

2.3.2 Potentiodynamic Polarization Scan With Respect To Exposure Time

Tafel law states that for high overpotentials, the relation between electrode potential and log of current density varies linearly. However, at steady state the anodic and cathodic reaction

rates are generally minimum, therefore that potential is referred as open circuit potential (Ecorr). The potential of the working electrode is varied using the predetermined scan rate and change in current is measured from cathodic to anodic directions from Ecorr. Thus the current density could be expressed as the function of overpotential[102–104].

$$\eta = a + b \log i$$

where η represents corrosion potential (Ecorr), i represents net current density Icorr, a is constant, b represents the Tafel slope of anodic and cathodic branch are based on the direction of sweep from Ecorr.

We obtained the potentiodynamic polarization curves using the CS-coated coupons upon exposure to 3.5 wt. % NaCl solution and were scanned between potential range from -0.9 to -0.1 volts with a scan rate of 1mv/sec. Figure 2.2 shows the potentiodynamic polarization scans for two conditions chosen (i) immediate and (ii) 2 hours wait, at room temperature. As shown in figure 2.2, the corrosion potential for the as-received coupon is -662 mV, whereas as the exposure time to the cold spray coating was increased for about 2 hours in 3.5 w.t. % NaCl solution, the corrosion potential increases to -657 mV respectively, which is slightly higher than that of the as-received coupon. Previous studies have also reported that for AA 6061 in chloride medium, the open circuit potential was comparable [105][106]. Therefore, the corrosion potential is not affected by the length of exposure time.

We can observe from figure 2.2 that the shape of the cathodic branch and anodic branch are almost similar, whereas the current density in the cathodic region has reduced by almost one order of magnitude for two hours exposure time. This means that increased exposure time led to a more stable passive film on the CS coated surface[107]. However, as the exposure time increased more oscillations/ sharp increase in current density could be observed in the anodic

region. This increase in current density provides a validation that the surface reactions taking place. The corrosion potential also moves slightly towards the active direction and thus lowering the corrosion resistance. Thus, providing us with an indication that the CS surface became more reactive and thus more prone to corrosion.

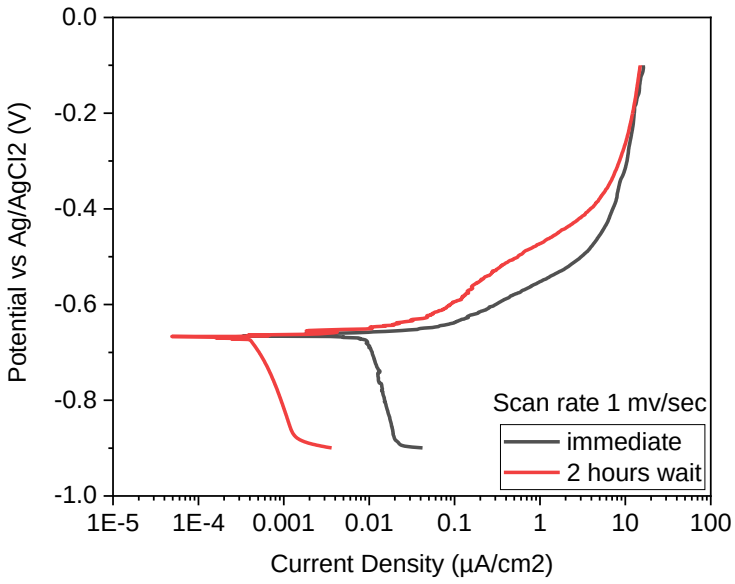

Figure 2.2 Potentiodynamic polarization curves of CS AA6061 coated on AA2024 coupons in 3.5wt. % solution using 1mV/sec scan rate (i) immediately upon exposure and (ii) 2 hours wait in 3.5% NaCl solution.

Table 2.3: Electrochemical parameters obtained using Tafel extrapolation method.

	Icorr (µA/cm^2)	**Ecorr (V)**	**Scan Rate**
Immediate	7.1	-662	1mV/sec
2 hours wait	1.0	-657	1mV/sec

Using this basis, the electrochemical parameters such as Icorr and Ecorr were obtained from the potentiodynamic polarization data using the Tafel extrapolation method and are summarized in table 2.2, respectively. In table 2.3, the Icorr value for a 2-hour wait decreases rapidly compared to the immediate exposure. This indicates that the longer the exposure time, the CS coating becomes more passive to corrosion. In the literature[108], when the corrosion potential of the metal increases with time, the growth of the passive film occurs on the surface, which slows down the corrosion process.

2.3.3 Measurement Of Force Per Width During Open Circuit Potential Condition

Figure 2.3 shows the force per width measurement performed during the open circuit potential, i.e., no external current or voltage was applied during this measurement. The force per width change was measured using the phase shifting curvature interferometry technique, which shows that the nature of force measured is compressive. This compressive force is in the range of 130 ± 80 N/m and reaches a stable value. It is evident from the results obtained that the stress development indicates corrosion of the cold spray coating when exposed to naturally aerated 3.5 wt—% NaCl solution. Many researchers in the literature have attributed the compressive stress due to the difference in coefficient of thermal expansion(CTE) of coating and substrate material[63,109,110]. The high-kinetic impact of the cold spray particles also causes a more prominent and deeper plastic region in cold spray coating leading to peening dominant condition[76,100]. Thus, indicating either the dissolution of tensile loaded material or formation of the chemical product on the surface, which is larger in volume when compared to the reactants.

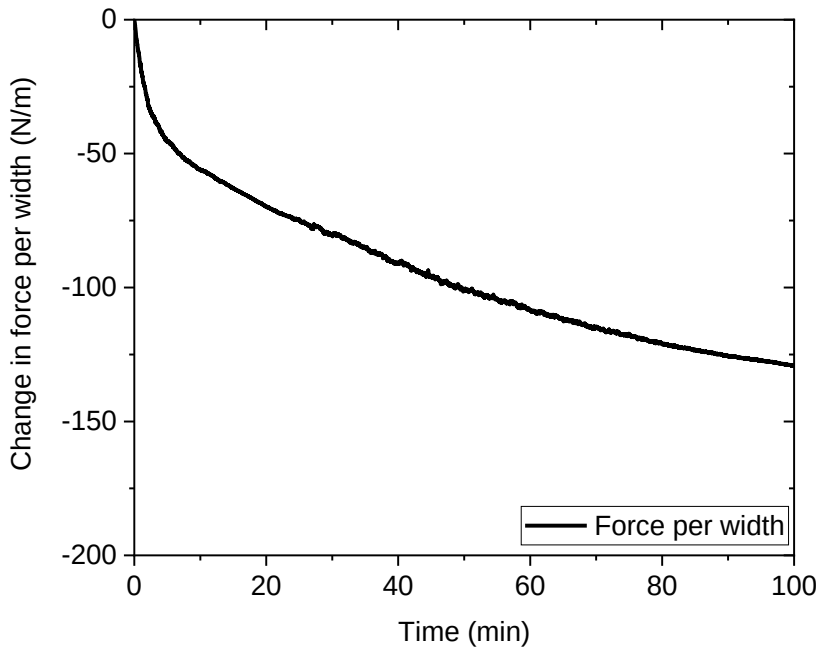

Figure 2.3 Change in force along the width during open circuit potential(OCP) scan for AA 2024.

2.3.4. In-Situ Stress Measurement During Anodic Dissolution At 0.3v Above OCP With Respect To Exposure Time

Figure 2.4 displays the in-situ stress measurements to study the relationship between force per width change and evolution of current density as a function of time at two different exposure conditions: (a) immediate and (b) two hours wait, upon polarizing the potential in the positive direction, i.e., +0.3 V above OCP. The solid black lines refer to force per width axis and dotted red lines refer to current density axis. In figure 2.4(a), during immediate exposure as the current density initiates, a tapered profile followed by spikes and jumps showing the passivation of slower corrosion behavior kinetics; however, the force per width increases steadily in the compressive direction immediately after exposure to the 3.5 wt.% NaCl solution.. The force per unit width shows a compressive behavior, representing a stable passive layer formation, which is

not directly attacked due to immediate exposure of electrolyte, thus causing less dissolution of tensile loaded material.

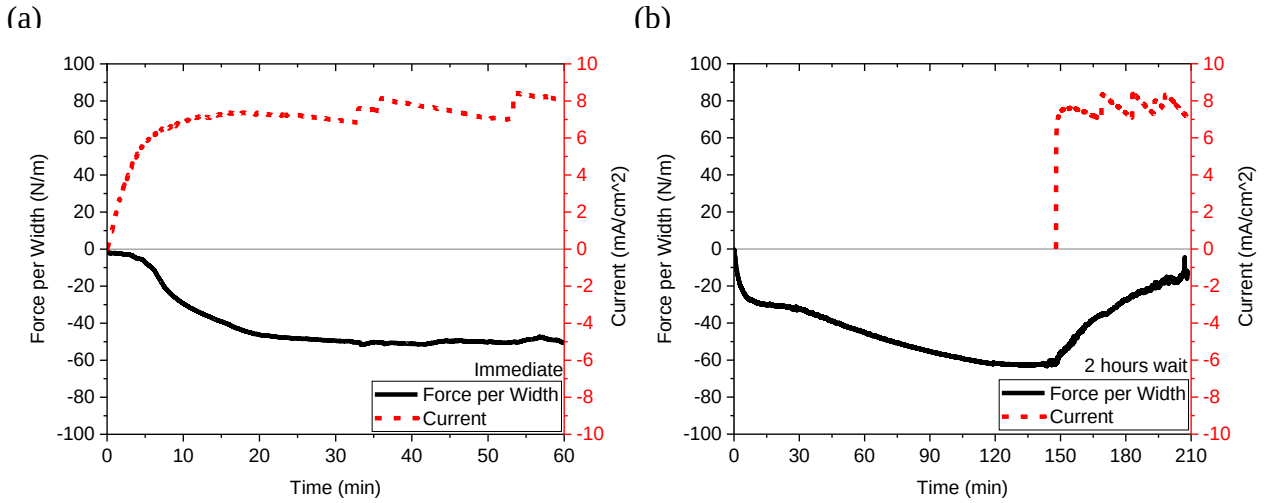

Figure 2.4 Force per width (black) and current density (dotted red) during Potentiostatic polarization scan at 0.3V above OCP for (a) immediate and (b) 2 hrs. wait.

On the other hand, when the exposure time to the surface was around 2 hours wait condition (fig 2.4(b)), the current density shows a rapid rise and more aggressive spikes and jumps. The force per width was increasing steadily in the compressive direction for almost 2 hours during OCP condition. As the anodic dissolution was performed, the force changed its direction, and thus tensile change was obtained during the measurement time of 60 mins. Because of longer exposure time, the passivation layer becomes unstable, leading to exposure of new surfaces, dissolution of the passive film, and ejection of particles reaching a maximum current of 8.4 mA/cm^2, thus providing inadequate corrosion protection. The ongoing exposure has led to the dissolution of the tensile-loaded material, and thus the subsequent anodic dissolution of tensile-loaded material causes the localized material dissolution simultaneously. In addition, evidence for higher current density was observed due to delay and presence of 3.5 wt.% NaCl solution.

2.3.5 Corroded Surface After Electrochemical Measurements

The backscattered SEM micrographs of the CS AA6061 coating on AA 2024 substrate after anodic dissolution at -0.3V above open circuit potential immersed for 1 hour are shown in figure 2.5, respectively. Fig 2.5(a) clearly shows the top view of the CS AA 6061 coating corroded region showing evidence of localized non-homogeneous corrosion as well as complete particle erosion at certain areas providing evidence of brittle fracture. The CS AA 6061 particles boundaries and surface area covered with the film are referred to as corrosion products (grey area). These corrosion products show the formation of pitting of spherical particles at the junction of grain boundaries, and pits with reaction products showing mud cracks formation after drying of the surface [111][112][14]. These sites show active nucleation regions for cracks forming an inhomogeneous network of branching due to attack on the grain boundary of the CS AA6061 coating. The pits formed on the CS AA6061 coating are small, have a rounded mouth shape, and various sizes represent complete particle ejection on the top surface, showing the underlying layer of CS AA6061 coating[113][114].

Fig 2.5(b) presents an estimation of the depth of the pits formed on the cross-section area of the surface. The maximum depth of attack was observed to be around 100 μm. The pits have small openings but a large cross-section area below the surface. These shapes are similar to the particle indication progress in along the inter-particle boundaries.

The cross-section view shows that the surface might be prone to pitting corrosion on the CS AA6061 coating upon exposure to 3.5 wt % NaCl solution. As the AA 6061 powder particles are ejected from the surface, as observed in fig 2.5(a), crack propagation was observed below the top surface, causing the corrosion products to peel off, as shown in fig 2.5(b)[115]. It can thus be

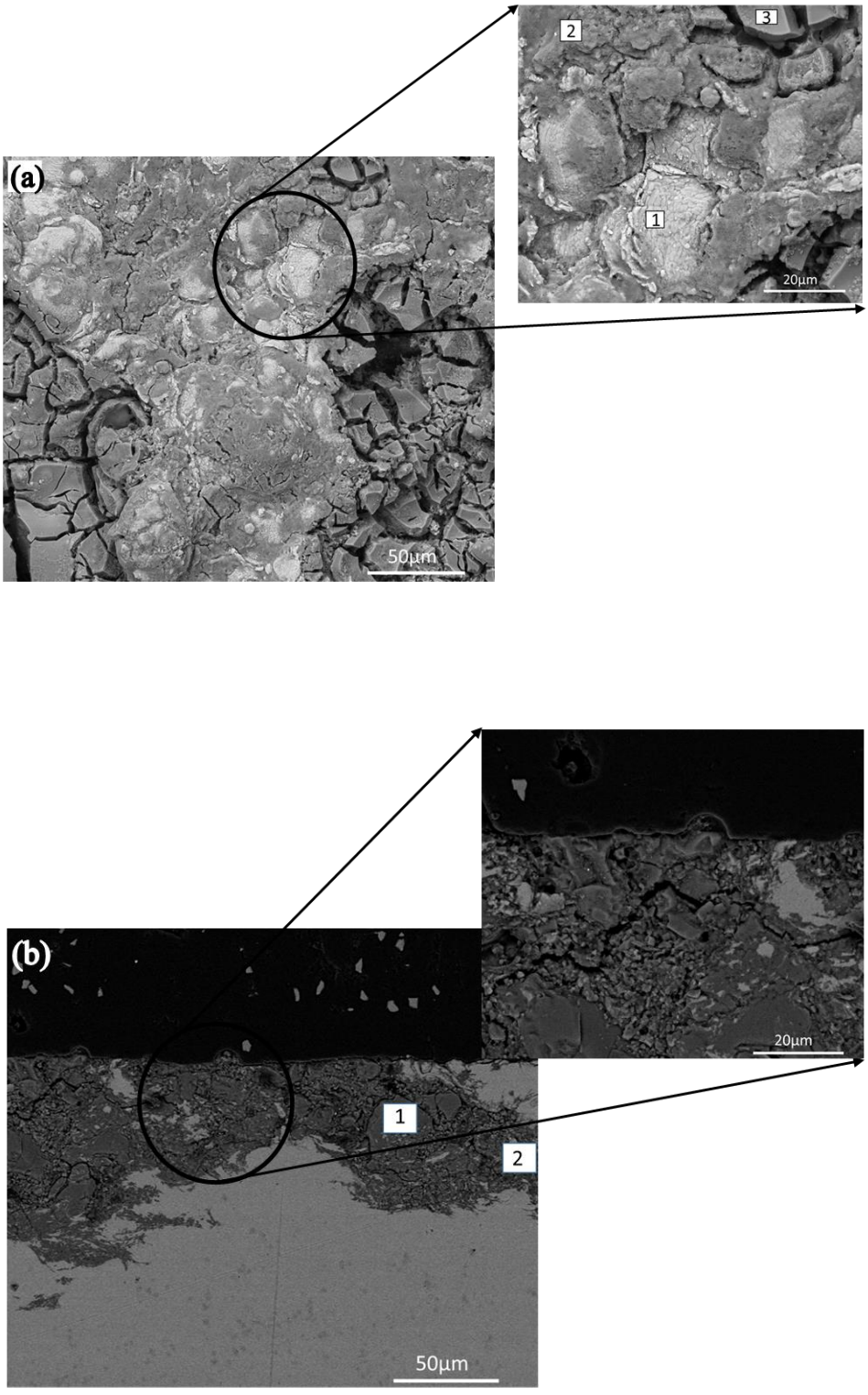

Figure 2.5 SEM micrograph of AA6061 cold spray coating on AA2024 substrate after anodic dissolution condition (a) top view (b) cross section view (crack propogation)

postulated that the outer layer seems protective but could rupture due to a network of cracks joining below the top surface layer. Presence of Cl^- ions in the 3.5 wt % NaCl solution along with tensile loaded material [116] on the surface could have penetrated inside the CS coating susceptible to corossion. Previous research has shown that the corrosion product formation tends to increase in volume due to corrosion products. This would lead to expansion and thus exposure of the underlying material[117], representing a pit formation and consequently a catastrophic failure.

2.3.6 Comparison Of Cold Spray Coating After Exposure Using Energy Dispersive X-Ray Analysis

Fig 2.6 shows the SEM EDS micrographs revealing the elemental chemical composition for the corroded surface as seen in fig 2.6, respectively. Fig 2.6(a) shows the EDS analysis of the top surface at three different regions. AA 6061 is a corrosive-resistant metal with the major constituents being Al-Mg-Si. Region 1 shows the area below the top layer of CS coating, revealing that the region below has higher aluminum content. Region 2 shows that CS particle boundaries on the corroded surface are rich in silicon and oxygen; however, minimal silicon content was present in the center of AA 6061 particles. This solute segregation could be attributed due to exposure of 3.5 wt.% NaCl solution during the corrosion experiment. Region 3 shows that the pit surfaces are covered with Si rich corroded material and exhibits rich sodium, oxygen, and carbon content. An increase in oxygen and chlorine content could have initiated local corrosion, which we can see in mud cracks-like morphology.

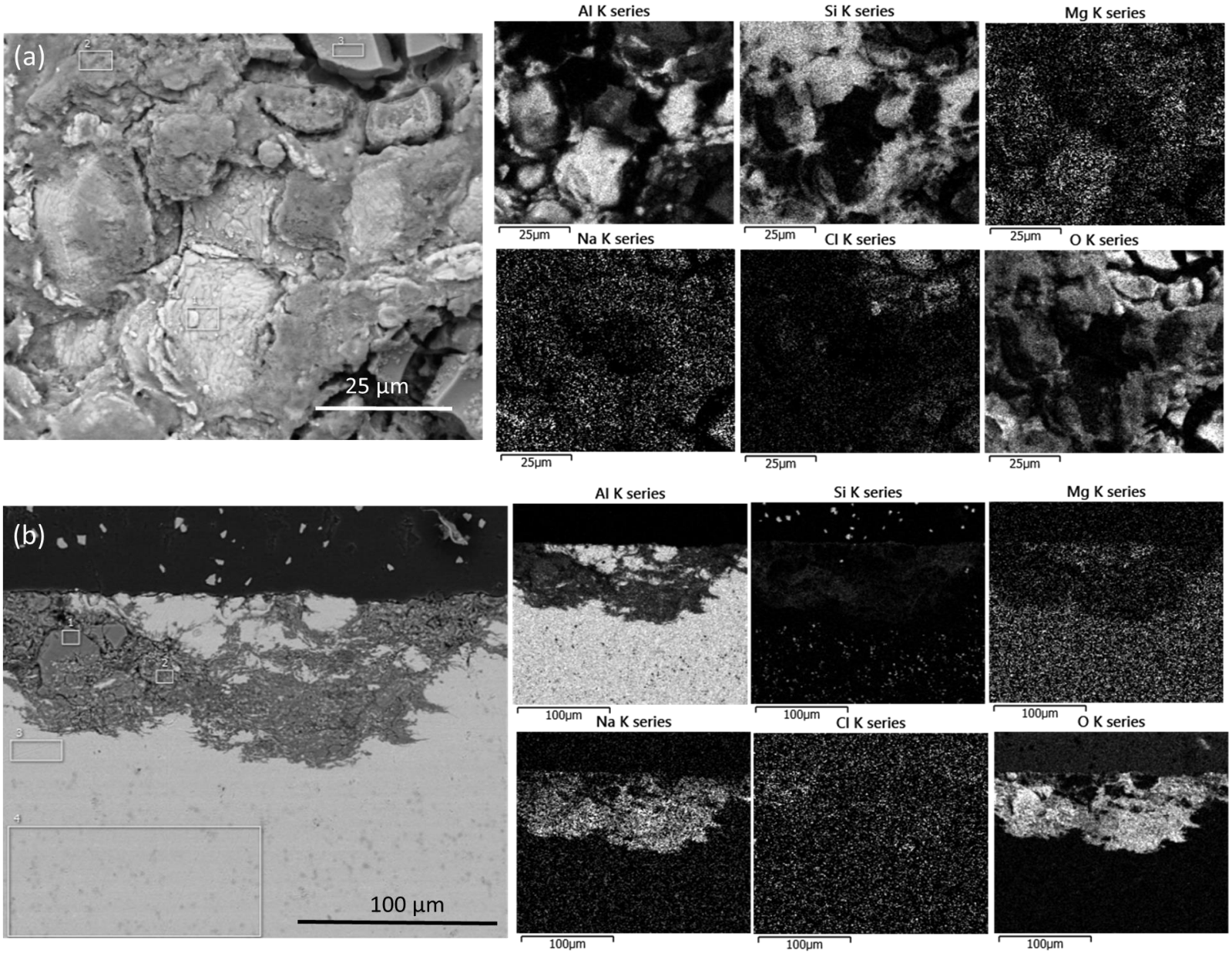

Figure 2.6 Energy-dispersive X-ray spectroscopy (EDS) maps of the cold spray coating showing the elemental maps distribution for Al, Si, Mg, Na, Cl and O (a) top view (b) cross section view

Fig 2.6(b) shows the EDS analysis of the cross-section area of the corroded cold spray coating. The corroded surface is richer in sodium and oxygen content, whereas silicon depletion occurs at the corroded area, and rich silicon content was found below the corroded surface. Previous studies [118–120] have reported the initiation of intergranular corrosion(IGC) due to the presence of higher silicon content in the matrix. EDS SEM analysis reveals that the presence of impurities at the grain boundaries may influence in degrading of the corrosion-resistant properties of CS AA 6061 particles. This may be due to the formation of intermetallic phases in the microstructure, causing degradation of the surface [121][105]. Thus, the results suggest that using CS AA 6061 coating may lead to corrosion.

2.4 Supplementary Information

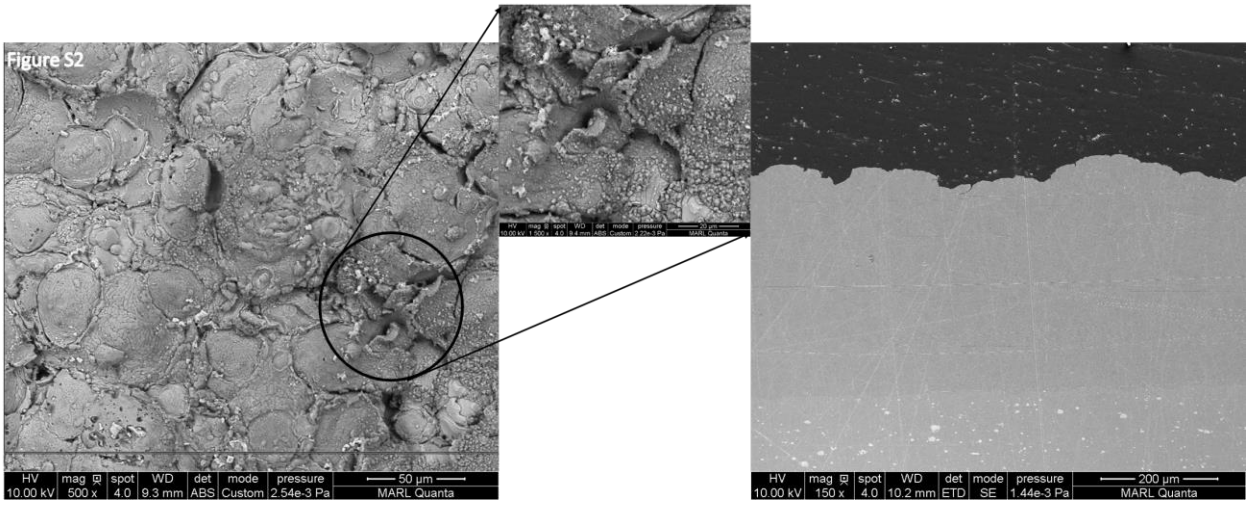

Figure S1: SEM micrograph for the as received CS coating exposed to naturally aerated 3.5 wt % NaCl solution for 24 hours (a) top view showing on left on the border of the corroded area and (b) cross section area on right.

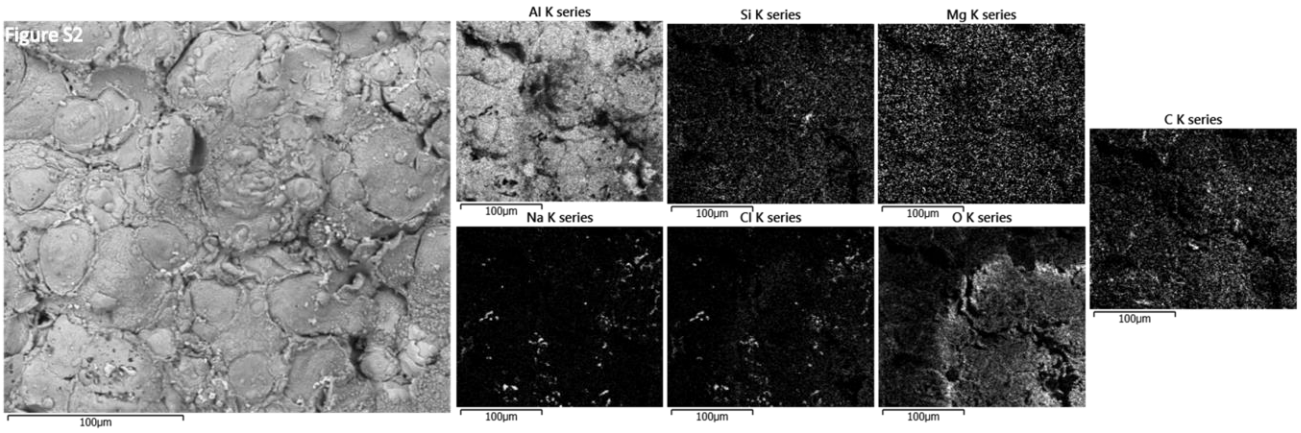

Figure S2: Energy-dispersive X-ray spectroscopy (EDS) maps of the cold spray coating showing the elemental maps distribution for Al, Si, Mg, Na, Cl and O (a) top view on the border of the corroded area.

SEM imaging of exposed coupons to 3.5 wt % NaCl solution provides evidence of no film formation; therefore, the stress development is most likely due to the dissolution of the tensile loaded material, causing the material to relax. Upon investigation of the 24 hours dipped coupons, using EDS,it was observed that the enrichment of Na, Cl, O, and Si was observed in Fig S3 which could be analyzed as forming an oxide layer on the surface. An interesting thing to observe is the effect of silicon enriching region, whereas the amount of silicon present in the alloy is less than 1%. EDS analysis of the solid particles for as received condition reveals that oxygen content is more in the particle boundaries than at the centre of the particles.

CHAPTER 3. CONCLUSION

3.1 General Conclusion

In this thesis work, we investigated the stress measurement and corrosion response of CS AA 6061 coating on AA 2024 substrate. The CS coating corrodes on exposure to 3.5wt.% NaCl solution. The potentiodynamic polarization test in 3.5 wt. % NaCl solution showed that the corrosion potential is not affected by the length of exposure time, however the current density significantly spikes as the exposure time is increased, causing a slight shift in open circuit potential, thus more prone to corrosion when exposed for a longer period. The corrosion current spikes increase, leading to the dissolution of the tensile-loaded material (i.e., CS AA 6061 coating) upon exposure to the surface with respect to time.

Insitu stress measurements along with the current density profile provide more evidence of superior corrosion characteristics depending upon the exposure time.Corrosion leads to the formation of Si-rich products at inter-particle boundaries, as well as deeper pits that have narrow openings but form a larger network below the surface. As deposited inter-particle boundary material is highly deformed. In addition, Si-rich from the particle center to the edges and formation of oxides due to iron depletion on the center, is responsible for accelerating the pitting corrosion. Because of the adsorption of the chlorine ions at the film solution interface.

The average depth of pits is roughly 100 μm, showing a small opening on the top but a larger cross-section below the surface. The crack propagates along the grain boundaries leading to catastrophic failures due to the formation of the underneath network.

Stress measurement suggests that initial exposure leads to the dissolution of tensile-loaded material and may be related to the formation of the Si-rich product found distributed over the surface. Variation in the Si content may be sensitizing the coated film for corrosion attack. Current

transients suggest fracture or removal of particles may be the signature of pit formation and deepening during anodic dissolution.

3.2 Future Work

Coatings via cold spray process is still an emerging field. In addition, there is always a room for exploring more avenues. In our experiments discussed in chapter 2, we studied CS coatings of similar material i.e. aluminum, however this work can be expanded to different materials to investigate the effect of coatings in variety of corrosive mediums and effect of residual stress on substrates such as copper and magnesium alloys.

There are other tests which can be performed to finalize the optimum parameters can be chose to minimize the effect of process variables on cold spray coatings. Some process variables include gas pressure, temperature, nozzle type, particles size chosen to obtain the best quality for cold spray coatings.

We were able to get some preliminary results for the force along the thickness on the substrate; however, another study could be performed is to study the effect of substrate with respect to variation of cold spray coating thickness. This study can be helpful to find the optimum thickness, which could be helpful to enhance the life of the real life application structure.

REFERENCES

[1] A. International, “Standard Terminology and Acronyms Relating to Corrosion”,ASTM International, West Conshohocken, PA, 2012. https://doi.org/10.1520/G0193-20A.2.

[2] G. Up, The Effects and Corrosion, Corrosion. (2000) 1–21.

[3] E. Bowman, G. Jacobson, G. Koch, J. Varney, N. Thopson, O. Moghissi, M. Gould, J. Payer, International Measures of Prevention, Application, and Economics of Corrosion Technologies Study, NACE International. (2016) A-19.

[4] A.F. Carreira, A.M. Pereira, E.P. Vaz, A.M. Cabral, T. Ghidini, L. Pigliaru, T. Rohr, Alternative corrosion protection pretreatments for aluminum alloys, Journal of Coatings Technology and Research. 14 (2017) 879–892. https://doi.org/10.1007/s11998-017-9922-9.

[5] R.I. Revilla, D. Verkens, T. Rubben, I. De Graeve, Corrosion and corrosion protection of additively manufactured aluminium alloys—a critical review, Materials. 13 (2020) 1–25. https://doi.org/10.3390/ma13214804.

[6] X. Li, X. Nie, L. Wang, D.O. Northwood, Corrosion protection properties of anodic oxide coatings on an Al-Si alloy, Surface and Coatings Technology. 200 (2005) 1994–2000. https://doi.org/10.1016/j.surfcoat.2005.08.019.

[7] G.W. Swain, M.P. Schultz, Protection of Marine Materials Class Notes, (1997).

[8] R.L. Twite, G.P. Bierwagen, Review of alternatives to chromate for corrosion protection of aluminum aerospace alloys, Progress in Organic Coatings. 33 (1998) 91–100. https://doi.org/10.1016/S0300-9440(98)00015-0.

[9] R.B.C. Cayless, ASM Handbook, Volume 2: Properties and Selection: Nonferrous Alloys and Special-Purpose Materials, 1990. https://doi.org/10.1361/asmhba000.

[10] A. Alloys, Understanding the Corrosion Behavior of Aluminum, 2020. https://doi.org/10.31399/asm.tb.caaa.t67870025.

[11] G.S. Chen, M. Gao, R.P. Wei, Microconstituent-Induced Pitting Corrosion in Aluminum Alloy 2024-T3, Corrosion (Houston). 52 (1996) 8–15. https://doi.org/10.5006/1.3292099.

[12] H. Ezuber, A. El-Houd, F. El-Shawesh, A study on the corrosion behavior of aluminum alloys in seawater, Materials and Design. 29 (2008) 801–805. https://doi.org/10.1016/j.matdes.2007.01.021.

[13] N. Birbilis, T.H. Muster, R.G. Buchheit, Corrosion of aluminum alloys, 2011. https://doi.org/10.3323/jcorr1991.45.166.

[14] Z. Szklarska-Smialowska, Pitting corrosion of aluminum, Corrosion Science. 41 (1999) 1743–1767. https://doi.org/10.1016/S0010-938X(99)00012-8.

[15] R.G. Buchheit, A Compilation of Corrosion Potentials Reported for Intermetallic Phases in Aluminum Alloys, Journal of The Electrochemical Society. 142 (1995) 3994–3996. https://doi.org/10.1149/1.2048447.

[16] R.J.K. Wood, Tribo-corrosion of coatings: A review, Journal of Physics D: Applied Physics. 40 (2007) 5502–5521. https://doi.org/10.1088/0022-3727/40/18/S10.

[17] P.A. Sørensen, S. Kiil, K. Dam-Johansen, C.E. Weinell, Anticorrosive coatings: A review, Journal of Coatings Technology and Research. 6 (2009) 135–176. https://doi.org/10.1007/s11998-008-9144-2.

[18] D. Tejero-Martin, M. Rezvani Rad, A. McDonald, T. Hussain, Beyond Traditional Coatings: A Review on Thermal-Sprayed Functional and Smart Coatings, Springer US, 2019. https://doi.org/10.1007/s11666-019-00857-1.

[19] F. Development, S. Coatings, [Woodhead Publishing series in metals and surface engineering no. 65] Espallargas, Nuria - Future development of thermal spray coatings _ types, designs, manufacture and applications (2015, Woodhead Publishing is a.pdf, n.d.

[20] C.P. Coatings, Metallurgical and Ceramic Protective Coatings, 1996. https://doi.org/10.1007/978-94-009-1501-5.

[21] H. Herman, Plasma Spray Deposition Processes, n.d.

[22] L.M. Berger, Application of hardmetals as thermal spray coatings, International Journal of Refractory Metals and Hard Materials. 49 (2015) 350–364. https://doi.org/10.1016/j.ijrmhm.2014.09.029.

[23] G. Barbezat, Advanced thermal spray technology and coating for lightweight engine blocks for the automotive industry, Surface and Coatings Technology. 200 (2005) 1990–1993. https://doi.org/10.1016/j.surfcoat.2005.08.017.

[24] C.U. Hardwicke, Y.C. Lau, Advances in thermal spray coatings for gas turbines and energy generation: A review, Journal of Thermal Spray Technology. 22 (2013) 564–576. https://doi.org/10.1007/s11666-013-9904-0.

[25] ISO/ASTM, Additive Manufacturing - General Principles Terminology (ASTM52900), 2013. https://www.iso.org/obp/ui/#iso:std:iso-astm:52900:dis:ed-2:v1:en (accessed June 27, 2021).

[26] D.L. Bourell, Perspectives on Additive Manufacturing, Annual Review of Materials Research. 46 (2016) 1–18. https://doi.org/10.1146/annurev-matsci-070115-031606.

[27] D. Herzog, V. Seyda, E. Wycisk, C. Emmelmann, Additive manufacturing of metals, Acta Materialia. 117 (2016) 371–392. https://doi.org/10.1016/j.actamat.2016.07.019.

[28] S. Yin, P. Cavaliere, B. Aldwell, R. Jenkins, H. Liao, W. Li, R. Lupoi, Cold spray additive manufacturing and repair: Fundamentals and applications, Additive Manufacturing. 21 (2018) 628–650. https://doi.org/10.1016/j.addma.2018.04.017.

[29] J.-P. Kruth, Material incress manufacturing by rapid prototyping techniques, (1991) 603–614. https://doi.org/10.1016/S0007-8506(07)61136-6.

[30] W.E. Frazier, Metal additive manufacturing: A review, Journal of Materials Engineering and Performance. 23 (2014) 1917–1928. https://doi.org/10.1007/s11665-014-0958-z.

[31] A. Zocca, P. Colombo, C.M. Gomes, J. Günster, Additive Manufacturing of Ceramics: Issues, Potentialities, and Opportunities, Journal of the American Ceramic Society. 98 (2015) 1983–2001. https://doi.org/10.1111/jace.13700.

[32] S. Bose, D. Ke, H. Sahasrabudhe, A. Bandyopadhyay, Additive manufacturing of biomaterials, Progress in Materials Science. 93 (2018) 45–111. https://doi.org/10.1016/j.pmatsci.2017.08.003.

[33] S. Mellor, L. Hao, D. Zhang, Additive manufacturing: A framework for implementation, International Journal of Production Economics. 149 (2014) 194–201. https://doi.org/10.1016/j.ijpe.2013.07.008.

[34] J. Holmström, J. Partanen, J. Tuomi, M. Walter, Rapid manufacturing in the spare parts supply chain: Alternative approaches to capacity deployment, Journal of Manufacturing Technology Management. 21 (2010) 687–697. https://doi.org/10.1108/17410381011063996.

[35] S.H. Huang, P. Liu, A. Mokasdar, L. Hou, Additive manufacturing and its societal impact: A literature review, International Journal of Advanced Manufacturing Technology. 67 (2013) 1191–1203. https://doi.org/10.1007/s00170-012-4558-5.

[36] S. Ford, M. Despeisse, Additive manufacturing and sustainability: an exploratory study of the advantages and challenges, Journal of Cleaner Production. 137 (2016) 1573–1587. https://doi.org/10.1016/j.jclepro.2016.04.150.

[37] M. Mehrpouya, A. Vosooghnia, A. Dehghanghadikolaei, B. Fotovvati, The benefits of additive manufacturing for sustainable design and production, INC, 2021. https://doi.org/10.1016/b978-0-12-818115-7.00009-2.

[38] T.S. Srivatsan, T.S. Sudarshan, Additive Manufacturing : Innovations, Advances, and Applications / Edited by T.S. Srivatsan, T.S. Sudarshan. 2016. Print., in: ProtoView, Beaverton: Ringgold, Inc, Beaverton, 2015: pp. 2–43.

[39] J.J. Lewandowski, M. Seifi, Metal Additive Manufacturing: A Review of Mechanical Properties, Annual Review of Materials Research. 46 (2016) 151–186. https://doi.org/10.1146/annurev-matsci-070115-032024.

[40] Y. Zhai, D.A. Lados, J.L. Lagoy, Additive Manufacturing: Making imagination the major Limitation, Jom. 66 (2014) 808–816. https://doi.org/10.1007/s11837-014-0886-2.

[41] A. Papyrin, V. Kosarev, S. Klinkov, A. Alkhimov, V.M. Fomin, Cold Spray Technology, Elsevier Science & Technology, Oxford, 2006.

[42] E. Irissou, J.G. Legoux, A.N. Ryabinin, B. Jodoin, C. Moreau, Review on cold spray process and technology: Part I - Intellectual property, Journal of Thermal Spray Technology. 17 (2008) 495–516. https://doi.org/10.1007/s11666-008-9203-3.

[43] V.K. Champagne, The cold spray materials deposition process: Fundamentals and applications, ASM International, 2007. https://doi.org/10.1533/9781845693787.

[44] A. Sova, S. Grigoriev, A. Okunkova, I. Smurov, Potential of cold gas dynamic spray as additive manufacturing technology, International Journal of Advanced Manufacturing Technology. 69 (2013) 2269–2278. https://doi.org/10.1007/s00170-013-5166-8.

[45] V.K. Champagne, D. Helfritch, P. Leyman, S. Grendahl, B. Klotz, Interface material mixing formed by the deposition of copper on aluminum by means of the cold spray process, Journal of Thermal Spray Technology. 14 (2005) 330–334. https://doi.org/10.1361/105996305X59332.

[46] H. Assadi, F. Gärtner, T. Stoltenhoff, H. Kreye, Bonding mechanism in cold gas spraying, Acta Materialia. 51 (2003) 4379–4394. https://doi.org/10.1016/S1359-6454(03)00274-X.

[47] E. Irissou, J.G. Legoux, B. Arsenault, C. Moreau, Investigation of Al-Al 2O 3 cold spray coating formation and properties, Journal of Thermal Spray Technology. 16 (2007) 661–668. https://doi.org/10.1007/s11666-007-9086-8.

[48] S.B. Dayani, S.K. Shaha, R. Ghelichi, J.F. Wang, H. Jahed, The impact of AA7075 cold spray coating on the fatigue life of AZ31B cast alloy, Surface and Coatings Technology. 337 (2018) 150–158. https://doi.org/10.1016/j.surfcoat.2018.01.008.

[49] N.B. Maledi, O.P. Oladijo, I. Botef, T.P. Ntsoane, A. Madiseng, L. Moloisane, Influence of cold spray parameters on the microstructures and residual stress of Zn coatings sprayed on mild steel, Surface and Coatings Technology. 318 (2017) 106–113. https://doi.org/10.1016/j.surfcoat.2017.03.062.

[50] Y.L. Liang, Z.B. Wang, J. Zhang, J.B. Zhang, K. Lu, Enhanced bonding property of cold-sprayed Zn-Al coating on interstitial-free steel substrate with a nanostructured surface layer, Applied Surface Science. 385 (2016) 341–348. https://doi.org/10.1016/j.apsusc.2016.05.142.

[51] H. Wu, X. Xie, M. Liu, C. Verdy, Y. Zhang, H. Liao, S. Deng, Stable layer-building strategy to enhance cold-spray-based additive manufacturing, Additive Manufacturing. 35 (2020) 101356. https://doi.org/10.1016/j.addma.2020.101356.

[52] A.W.Y. Tan, S. Wen, N.W. Khun, I. Marinescu, Z. Dong, E. Liu, Potential of cold spray as additive manufacturing for TI6AL4V, Proceedings of the International Conference on Progress in Additive Manufacturing. Part F1290 (2016) 403–408. https://doi.org/10.3850/2424-8967-V02-155.

[53] S. Bagherifard, S. Monti, M.V. Zuccoli, M. Riccio, J. Kondás, M. Guagliano, Cold spray deposition for additive manufacturing of freeform structural components compared to selective laser melting, Materials Science and Engineering A. 721 (2018) 339–350. https://doi.org/10.1016/j.msea.2018.02.094.

[54] S. Pathak, G.C. Saha, Development of sustainable cold spray coatings and 3D additive manufacturing components for repair/manufacturing applications: A critical review, Coatings. 7 (2017). https://doi.org/10.3390/coatings7080122.

[55] S. Bagherifard, J. Kondas, S. Monti, J. Cizek, F. Perego, O. Kovarik, F. Lukac, F. Gaertner, M. Guagliano, Tailoring cold spray additive manufacturing of steel 316 L for static and cyclic load-bearing applications, Materials and Design. 203 (2021) 109575. https://doi.org/10.1016/j.matdes.2021.109575.

[56] A. Vafadar, F. Guzzomi, A. Rassau, K. Hayward, Advances in metal additive manufacturing: A review of common processes, industrial applications, and current challenges, Applied Sciences (Switzerland). 11 (2021) 1–33. https://doi.org/10.3390/app11031213.

[57] J. Delgado, J. Ciurana, C.A. Rodríguez, Influence of process parameters on part quality and mechanical properties for DMLS and SLM with iron-based materials, International Journal of Advanced Manufacturing Technology. 60 (2012) 601–610. https://doi.org/10.1007/s00170-011-3643-5.

[58] P. Cavaliere, A. Silvello, Crack Repair in Aerospace Aluminum Alloy Panels by Cold Spray, Journal of Thermal Spray Technology. 26 (2017) 661–670. https://doi.org/10.1007/s11666-017-0534-9.

[59] A. Berzins, R.T. Lowson, K.J. Mirams, Aluminium corrosion studies. III* Chloride adsorption isotherms on corroding aluminium, Australian Journal of Chemistry. 30 (1977) 1891–1903. https://doi.org/10.1071/CH9771891.

[60] E.A. Starke, S. Mridha, Aluminum Alloys: Alloy, Heat Treatment, and Temper Designation, Reference Module in Materials Science and Materials Engineering. (2016). https://doi.org/10.1016/b978-0-12-803581-8.02553-4.

[61] V. Champagne, D. Helfritch, Critical Assessment 11: Structural repairs by cold spray, Materials Science and Technology (United Kingdom). 31 (2015) 627–634. https://doi.org/10.1179/1743284714Y.0000000723.

[62] Y. Xu, I.M. Hutchings, Cold spray deposition of thermoplastic powder, Surface and Coatings Technology. 201 (2006) 3044–3050. https://doi.org/10.1016/j.surfcoat.2006.06.016.

[63] X.T. Luo, C.X. Li, F.L. Shang, G.J. Yang, Y.Y. Wang, C.J. Li, High velocity impact induced microstructure evolution during deposition of cold spray coatings: A review, Surface and Coatings Technology. 254 (2014) 11–20. https://doi.org/10.1016/j.surfcoat.2014.06.006.

[64] W. Li, K. Yang, S. Yin, X. Yang, Y. Xu, R. Lupoi, Solid-state additive manufacturing and repairing by cold spraying: A review, Journal of Materials Science and Technology. 34 (2018) 440–457. https://doi.org/10.1016/j.jmst.2017.09.015.

[65] J. Karthikeyan, The advantages and disadvantages of the cold spray coating process, in: The Cold Spray Materials Deposition Process: Fundamentals and Applications, Elsevier Ltd., 2007: pp. 62–71. https://doi.org/10.1533/9781845693787.1.62.

[66] R. Morgan, P. Fox, J. Pattison, C. Sutcliffe, W. O'Neill, Analysis of cold gas dynamically sprayed aluminium deposits, Materials Letters. 58 (2004) 1317–1320. https://doi.org/10.1016/j.matlet.2003.09.048.

[67] M. Diab, X. Pang, H. Jahed, The effect of pure aluminum cold spray coating on corrosion and corrosion fatigue of magnesium (3% Al-1% Zn) extrusion, Surface and Coatings Technology. 309 (2017) 423–435. https://doi.org/10.1016/j.surfcoat.2016.11.014.

[68] L. Ajdelsztajn, B. Jodoin, G.E. Kim, J.M. Schoenung, Cold spray deposition of nanocrystalline aluminum alloys, Metallurgical and Materials Transactions A: Physical Metallurgy and Materials Science. 36 (2005) 657–666. https://doi.org/10.1007/s11661-005-0182-4.

[69] A.M. Vilardell, N. Cinca, A. Concustell, S. Dosta, I.G. Cano, J.M. Guilemany, Cold spray as an emerging technology for biocompatible and antibacterial coatings: state of art, Journal of Materials Science. 50 (2015) 4441–4462. https://doi.org/10.1007/s10853-015-9013-1.

[70] S. Rech, A. Trentin, S. Vezzù, E. Vedelago, J.G. Legoux, E. Irissou, Different Cold Spray Deposition Strategies: Single- and Multi-layers to Repair Aluminium Alloy Components, Journal of Thermal Spray Technology. 23 (2014) 1237–1250. https://doi.org/10.1007/s11666-014-0141-y.

[71] H. Assadi, T. Schmidt, H. Richter, J.O. Kliemann, K. Binder, F. Gärtner, T. Klassen, H. Kreye, On parameter selection in cold spraying, Journal of Thermal Spray Technology. 20 (2011) 1161–1176. https://doi.org/10.1007/s11666-011-9662-9.

[72] J.D. Majumdar, I. Manna, Development of functionally graded coating by thermal spray deposition, 2015. https://doi.org/10.4018/978-1-4666-7489-9.ch005.

[73] R. Ghelichi, S. Bagherifard, D. Macdonald, I. Fernandez-Pariente, B. Jodoin, M. Guagliano, Experimental and numerical study of residual stress evolution in cold spray coating, Applied Surface Science. 288 (2014) 26–33. https://doi.org/10.1016/j.apsusc.2013.09.074.

[74] K. Yang, W. Li, P. Niu, X. Yang, Y. Xu, Cold sprayed AA2024/Al2O3 metal matrix composites improved by friction stir processing: Microstructure characterization, mechanical performance and strengthening mechanisms, Journal of Alloys and Compounds. 736 (2018) 115–123. https://doi.org/10.1016/j.jallcom.2017.11.132.

[75] N. Li, W. Li, X. Yang, Y. Xu, A. Vairis, Corrosion characteristics and wear performance of cold sprayed coatings of reinforced Al deposited onto friction stir welded AA2024-T3 joints, Surface and Coatings Technology. 349 (2018) 1069–1076. https://doi.org/10.1016/j.surfcoat.2018.06.058.

[76] G. Shayegan, H. Mahmoudi, R. Ghelichi, J. Villafuerte, J. Wang, M. Guagliano, H. Jahed, Residual stress induced by cold spray coating of magnesium AZ31B extrusion, Materials and Design. 60 (2014) 72–84. https://doi.org/10.1016/j.matdes.2014.03.054.

[77] D.J. Greving, E.F. Rybicki, J.R. Shadley, Through-thickness residual stress evaluations for several industrial thermal spray coatings using a modified layer-removal method, Journal of Thermal Spray Technology. 3 (1994) 379–388. https://doi.org/10.1007/BF02658983.

[78] R.C. McCune, W.T. Donlon, O.O. Popoola, E.L. Cartwright, Characterization of copper layers produced by cold gas-dynamic spraying, Journal of Thermal Spray Technology. 9 (2000) 73–82. https://doi.org/10.1361/105996300770350087.

[79] A. Moridi, S.M. Hassani-Gangaraj, M. Guagliano, S. Vezzu, Effect of Cold Spray Deposition of Similar Material on Fatigue Behavior of Al 6082 Alloy, in: C. Jay (Ed.), Fracture and Fatigue, Volume 7, Springer International Publishing, Cham, 2014: pp. 51–57.

[80] V. Luzin, K. Spencer, M.X. Zhang, Residual stress and thermo-mechanical properties of cold spray metal coatings, Acta Materialia. 59 (2011) 1259–1270. https://doi.org/10.1016/j.actamat.2010.10.058.

[81] J. Wang, P. Shrotriya, K.S. Kim, Surface residual stress measurement using curvature interferometry, Experimental Mechanics. 46 (2006) 39–46. https://doi.org/10.1007/s11340-006-5864-3.

[82] Ö.Ö. Çapraz, K.R. Hebert, P. Shrotriya, In Situ Stress Measurement During Aluminum Anodizing Using Phase-Shifting Curvature Interferometry, Journal of The Electrochemical Society. 160 (2013) D501–D506. https://doi.org/10.1149/2.025311jes.

[83] B. Marzbanrad, H. Jahed, E. Toyserkani, On the evolution of substrate's residual stress during cold spray process: A parametric study, Materials and Design. 138 (2018) 90–102. https://doi.org/10.1016/j.matdes.2017.10.062.

[84] R. Ghelichi, D. MacDonald, S. Bagherifard, H. Jahed, M. Guagliano, B. Jodoin, Microstructure and fatigue behavior of cold spray coated Al5052, Acta Materialia. 60 (2012) 6555–6561. https://doi.org/10.1016/j.actamat.2012.08.020.

[85] Y. Tao, T. Xiong, C. Sun, H. Jin, H. Du, T. Li, Effect of α-Al 2 O 3 on the properties of cold sprayed Al/α-Al 2 O 3 composite coatings on AZ91D magnesium alloy, Applied Surface Science. 256 (2009) 261–266. https://doi.org/10.1016/j.apsusc.2009.08.012.

[86] T. Proulx, Fracture and Fatigue , Volume 7, 2013.

[87] K. Mutombo, M. Du Toit, Corrosion fatigue behaviour of aluminium alloy 6061-T651 welded using fully automatic gas metal arc welding and ER5183 filler alloy, International Journal of Fatigue. 33 (2011) 1539–1547. https://doi.org/10.1016/j.ijfatigue.2011.06.012.

[88] K. Chanyathunyaroj, S. Phetchcrai, G. Laungsopapun, A. Rengsomboon, Fatigue characteristics of 6061 aluminum alloy subject to 3.5% NaCl environment, International Journal of Fatigue. 133 (2020) 105420. https://doi.org/10.1016/j.ijfatigue.2019.105420.

[89] M. Weber, P.D. Eason, H. Özdeş, M. Tiryakioğlu, The effect of surface corrosion damage on the fatigue life of 6061-T6 aluminum alloy extrusions, Materials Science and Engineering A. 690 (2017) 427–432. https://doi.org/10.1016/j.msea.2017.03.026.

[90] A. Amirat, A. Mohamed-Chateauneuf, K. Chaoui, Reliability assessment of underground pipelines under the combined effect of active corrosion and residual stress, International Journal of Pressure Vessels and Piping. 83 (2006) 107–117. https://doi.org/10.1016/j.ijpvp.2005.11.004.

[91] S. Ngai, T. Ngai, F. Vogel, W. Story, G.B. Thompson, L.N. Brewer, Saltwater corrosion behavior of cold sprayed AA7075 aluminum alloy coatings, Corrosion Science. 130 (2018) 231–240. https://doi.org/10.1016/j.corsci.2017.10.033.

[92] M.R. Rokni, C.A. Widener, V.R. Champagne, Microstructural evolution of 6061 aluminum gas-atomized powder and high-pressure cold-sprayed deposition, Journal of Thermal Spray Technology. 23 (2014) 514–524. https://doi.org/10.1007/s11666-013-0049-y.

[93] Z. Zhang, F. Liu, E.H. Han, L. Xu, Mechanical and corrosion properties in 3.5% NaCl solution of cold sprayed Al-based coatings, Surface and Coatings Technology. 385 (2020) 125372. https://doi.org/10.1016/j.surfcoat.2020.125372.

[94] Y.K. Wei, X.T. Luo, Y. Ge, X. Chu, G.S. Huang, C.J. Li, Deposition of fully dense Al-based coatings via in-situ micro-forging assisted cold spray for excellent corrosion protection of AZ31B magnesium alloy, Journal of Alloys and Compounds. 806 (2019) 1116–1126. https://doi.org/10.1016/j.jallcom.2019.07.279.

[95] M.R. Rokni, C.A. Widener, G.A. Crawford, M.K. West, An investigation into microstructure and mechanical properties of cold sprayed 7075 Al deposition, Materials Science and Engineering A. 625 (2015) 19–27. https://doi.org/10.1016/j.msea.2014.11.059.

[96] L. Liu, Y. Li, F. Wang, Influence of grain size on the corrosion behavior of a Ni-based superalloy nanocrystalline coating in NaCl acidic solution, Electrochimica Acta. 53 (2008) 2453–2462. https://doi.org/10.1016/j.electacta.2007.10.048.

[97] M.R. Bothwell, Galvanic Relationships between Aluminum Alloys and Magnesium Alloys, Journal of The Electrochemical Society. 106 (1959) 1019. https://doi.org/10.1149/1.2427201.

[98] D. Yavas, A. Alshehri, P. Mishra, P. Shrotriya, A.F. Bastawros, K.R. Hebert, Morphology and stress evolution during the initial stages of intergranular corrosion of X70 steel, Electrochimica Acta. 285 (2018) 336–343. https://doi.org/10.1016/j.electacta.2018.07.207.

[99] M.R. Ardigo, M. Ahmed, A. Besnard, Stoney formula: Investigation of curvature measurements by optical profilometer, Advanced Materials Research. 996 (2014) 361–366. https://doi.org/10.4028/www.scientific.net/AMR.996.361.

[100] T. Suhonen, T. Varis, S. Dosta, M. Torrell, J.M. Guilemany, Residual stress development in cold sprayed Al, Cu and Ti coatings, Acta Materialia. 61 (2013) 6329–6337. https://doi.org/10.1016/j.actamat.2013.06.033.

[101] M.R. Rokni, C.A. Widener, V.R. Champagne, Microstructural stability of ultrafine grained cold sprayed 6061 aluminum alloy, Applied Surface Science. 290 (2014) 482–489. https://doi.org/10.1016/j.apsusc.2013.11.127.

[102] E. McCafferty, Validation of corrosion rates measured by the Tafel extrapolation method, Corrosion Science. 47 (2005) 3202–3215. https://doi.org/10.1016/j.corsci.2005.05.046.

[103] B.N. Popov, Basics of Corrosion Measurements, Corrosion Engineering. (2015) 181–237. https://doi.org/10.1016/b978-0-444-62722-3.00005-7.

[104] X.L. Zhang, Z.H. Jiang, Z.P. Yao, Y. Song, Z.D. Wu, Effects of scan rate on the potentiodynamic polarization curve obtained to determine the Tafel slopes and corrosion current density, Corrosion Science. 51 (2009) 581–587. https://doi.org/10.1016/j.corsci.2008.12.005.

[105] W.A. Badawy, F.M. Al-Kharafi, A.S. El-Azab, Electrochemical behaviour and corrosion inhibition of Al, Al-6061 and Al-Cu in neutral aqueous solutions, Corrosion Science. 41 (1999) 709–727. https://doi.org/10.1016/S0010-938X(98)00145-0.

[106] D. V. Dzhurinskiy, S.S. Dautov, P.G. Shornikov, I.S. Akhatov, Surface modification of aluminum 6061-O Alloy by plasma electrolytic oxidation to improve corrosion resistance properties, Coatings. 11 (2021) 1–13. https://doi.org/10.3390/coatings11010004.

[107] S.L. De Assis, S. Wolynec, I. Costa, Corrosion characterization of titanium alloys by electrochemical techniques, Electrochimica Acta. 51 (2006) 1815–1819. https://doi.org/10.1016/j.electacta.2005.02.121.

[108] S. Hiromoto, Corrosion of metallic biomaterials, in: Metals for Biomedical Devices, Woodhead Publishing, 2010: pp. 99–121. https://doi.org/10.1533/9781845699246.2.99.

[109] P.D. Reena Kumari, J. Nayak, A. Nityananda Shetty, Corrosion behavior of 6061/Al-15 vol. pct. SiC(p) composite and the base alloy in sodium hydroxide solution, Arabian Journal of Chemistry. 9 (2016) S1144–S1154. https://doi.org/10.1016/j.arabjc.2011.12.003.

[110] S. Kuroda, T. Fukushima, S. Kitahara, Simultaneous measurement of coating thickness and deposition stress during thermal spraying, Thin Solid Films. 164 (1988) 157–163. https://doi.org/10.1016/0040-6090(88)90127-7.

[111] S. Shamsudeen, E.R.D. John, Effect of welding on pitting and intergranular corrosion behavior of marine grade aluminum alloy, Materials Performance and Characterization. 8 (2019) 555–570. https://doi.org/10.1520/MPC20180118.

[112] J. Cabral-Miramontes, C. Gaona-Tiburcio, F. Estupinán-López, M. Lara-Banda, P. Zambrano-Robledo, D. Nieves-Mendoza, E. Maldonado-Bandala, J. Chacón-Nava, F. Almeraya-Calderón, Corrosion resistance of hard coat anodized AA 6061 in citric-sulfuric solutions, Coatings. 10 (2020) 1–14. https://doi.org/10.3390/COATINGS10060601.

[113] M. Ramachandra, K. Radhakrishna, Sliding wear, slurry erosive wear, and corrosive wear of aluminium/SiC composite, Materials Science- Poland. 24 (2006) 333–349.

[114] H.C. Ananda Murthy, V. Bheema Raju, C. Shivakumara, Effect of TiN particulate reinforcement on corrosive behaviour of aluminium 6061 composites in chloride medium, Bulletin of Materials Science. 36 (2013) 1057–1066. https://doi.org/10.1007/s12034-013-0560-2.

[115] N. Vu Nguyen, P. Li, Fatigue behaviour of AA6061-T6 alloys in the corrosive environment, MATEC Web of Conferences. 165 (2018) 1–6. https://doi.org/10.1051/matecconf/201816503015.

[116] Y. Murakami, Stress-Corrosion Cracking of Aluminum Alloys, Journal of Japan Institute of Light Metals. 31 (1981) 748–757. https://doi.org/10.2464/jilm.31.748.

[117] M.J. Robinson, The role of wedging stresses in the exfoliation corrosion of high strength aluminium alloys, Corrosion Science. 23 (1983) 887–899. https://doi.org/10.1016/0010-938X(83)90016-1.

[118] T. Haruna, T. Kouno, S. Fujimoto, Electrochemical conditions for environment-assisted cracking of 6061 Al alloy, Corrosion Science. 47 (2005) 2441–2449. https://doi.org/10.1016/j.corsci.2004.10.011.

[119] G. Svenningsen, M.H. Larsen, J.C. Walmsley, J.H. Nordlien, K. Nisancioglu, Effect of artificial aging on intergranular corrosion of extruded AlMgSi alloy with small Cu content, Corrosion Science. 48 (2006) 1528–1543. https://doi.org/10.1016/j.corsci.2005.05.045.

[120] K.M. Fleming, A. Zhu, J.R. Scully, Corrosion of AA6061 brazed with an Al-Si alloy: Effects of Si on metallurgical and corrosion behavior, Corrosion. 68 (2012) 1126–1145. https://doi.org/10.5006/0677.

[121] L.H. Pereira, G.H. Asato, L.B. Otani, A.M. Jorge, C.S. Kiminami, C. Bolfarini, W.J. Botta, Changing the solidification sequence and the morphology of iron-containing intermetallic phases in AA6061 aluminum alloy processed by spray forming, Materials Characterization. 145 (2018) 507–515. https://doi.org/10.1016/j.matchar.2018.09.006.